Studying on Optimization of Construction Cable Force of Asymmetric Fish-Shuttle-Shaped Single Tower Cable-Stayed Bridge

Zhiming Wang[1], Wenshu Sun[1], Shunan Yao[2], Zhiyong Yang[3], Jian Wang[3,*], Jiankun Liu[3]

[1] CSCEC4 Civil Engineering Co., Ltd., Shenzhen 518052, China
[2] China Construction Infrastructure Corp., Ltd., Beijing 100089, China
[3] School of Civil Engineering, Sun Yat-sen University, Guangzhou 510275, China

*Corresponding author, Jian Wang,
E-mail: wangj833@mail.sysu.edu.cn

Abstract. The emergence of asymmetric cable-stayed bridges with different shape of main tower poses a number of challenges for analysis of construction cable force. In this paper, based on an asymmetric fish-shuttle-shaped single tower cable-stayed bridge in China, finite element software Midas Civil was adopted to build the model of the bridge. The unstressed state method was used to optimize the construction cable forces of the bridge, and its reasonable construction state was determined. Results indicated that the cable forces under construction calculated completed bridge internal force state ranged from 2620.5 to 6913.1kN, which was slightly reduced overall compared with that under target completed bridge internal force state, assuring the steady and safety of cables during construction. Maximum difference of 6.00% between the cable forces under target completed bridge internal force state and construction calculated completed bridge internal force state. The average error of the cable forces of the whole bridge was 1.41%, among which the average error of 0.99% of the main-span cable forces and 1.83% of the side-span cable forces. That is to say, through an effective tensioning could ensure that the error of construction completed bridge cable forces of the bridge with a span of nearly 400 m was small. In addition, the use of unstressed state method to optimize the cable-stayed bridge construction force could better meet the construction requirements. The maximum stresses of main tower, side-span concrete girders and main-span steel box girders at each construction stage were 23.0, 6.6, and 120.5 MPa, respectively, which was significantly lower than the design strength of corresponding concrete and steel, showing the safety of structural stress state of cable-stayed bridge. The maximum displacements of main tower, side-span concrete girders and main-span steel box girders at each construction stage were 156.5, 20.8, and 1206.4 mm, respectively, which could be ignored compared with the structural dimension and layout, indicating a reasonable structural construction deformation of cable-stayed bridge. The research results can provide reference value for the design and optimization of similar projects.

W. Nie et al. (eds.), *Proceedings of the 2024 6th International Conference on Hydraulic, Civil and Construction Engineering (HCCE 2024)*, Atlantis Highlights in Engineering 37,
https://doi.org/10.2991/978-94-6463-726-7_36

Keywords: Asymmetric cable-stayed bridge, fish-shuttle-shaped main tower, optimization of construction cable force, unstressed state method, finite element analysis

1 Introduction

With the rapid development of the global economy, large-scale urbanization is unfolding worldwide, and people's demands for bridge span, cost-effectiveness, and aesthetics are also increasing. The cable-stayed bridges are characterized in its high overall stiffness, strong wind resistance, large spanning capacity, diverse structural forms, and aesthetic appeal, which have become one of the fastest-developing and most competitive bridges in the world today [1-2]. Cable-stayed bridges are a higher-order statically indeterminate structural system composed of three basic components, including inclined stay cables, towers, and stiffening girders [3]. Since the completion of the first modern cable-stayed bridge, the Stromsund Bridge, in 1956 [4], cable-stayed bridges have been rapidly developing around the world. To date, cable-stayed bridges have achieved historic advancements in long spans, ultra-long spans, and composite structural systems [5], such as the Yavuz Sultan Selim Bridge (Turkey, 1408 m), the Russky Island Bridge (Russia, 1104 m), and the Sutong Yangtze River Bridge (China, 1088 m). At the same time, the rapid development of modern construction technology and architectural aesthetics has led to the emergence of various cable-stayed bridges with beautiful appearances and diverse forms around the world, which can be classified in multiple ways based on different factors [6]. For example, based on the number of towers, cable-stayed bridges can be classified into single-tower, double-tower, and multi-tower cable-stayed bridges; according to the shape of the towers, they can be divided into vertical tower, inclined tower, and irregularly shaped tower, etc. The towers of asymmetric single tower cable-stayed bridges can be flexibly positioned on the side with favorable geological conditions, which not only reduces construction difficulty but also lowers construction costs [7]. In addition, irregularly shaped tower cable-stayed bridges, due to their unique appearance and strong adaptability to the terrain and environment, often become iconic landmarks in cities and are more popular. Especially, the fish-shuttle-shaped main towers not only have a streamlined appearance, but also can be integrated with the natural environment, which in turn enhances the visual impact and artistic value of the bridge. This design concept has been increasingly emphasized in modern cities, and can enhance the cultural and tourism attractiveness of the city. Therefore, asymmetric fish-shuttle-shaped single tower cable-stayed bridges have greater engineering application value.

However, the structural response of asymmetric irregular single tower cable-stayed bridges may be significantly different from that of conventional bridges when responding to complex loads. Especially, when the main tower is in the shape of a fish shuttle, and there is a significant inhomogeneity in the stiffness of the cable-stayed bridge structure, which leads to a more complex force situation in the tower when subjected to loads. Therefore, the optimization of construction cable forces is particularly crucial when designing the cable-stayed bridge. The structural system and the tensions of cable-stayed bridges change continuously throughout the construction process. At the same time, the nonlinear behavior of the structure can cause deviations of the final completed bridge cable forces and the cable profile differing from the intended design requirements. Therefore, it is crucial to determine how to ensure construction cable forces and predict the following cable forces during construction, making sure the final completed cable forces meet the requirements [8]. In recent years, researchers have proposed various optimization methods for cable forces during construction based on theoretical research and engineering practice, including reverse construction method [9], forward installation iterative method [10], reverse construction-forward installation iterative method [11], and the unstressed state method [12-13], etc. The methods above have advantages in clear mechanical conceptions and optimization targets, which have demonstrated their applicability on different types of cable-stayed bridges. The optimization questions of cable forces of asymmetric irregularly shaped tower cable-stayed bridges have become a hot topic, which appeal numerous researchers to carry out a large number of related studies. Yu [14] adopted forward installation iterative method to optimize the cable forces during construction of an asymmetric '1'-shaped single tower cable-stayed bridge. Results indicated that the errors of 4 group of cables all arrived 0% after five iterations, suggesting that the application of forward installation iterative method was remarkable. Liu [15] optimized the cable forces during construction of an asymmetric pagoda-shaped single tower cable-stayed bridge by using reverse construction-forward installation iterative method. Results suggested that the optimized cable forces during construction can meet the structural forces and geometric shape requirements during the construction process. Wang et.al. [16] and Xiao [17] optimized the cable forces during construction of an asymmetric double-column-sail-shaped and 'H'-shaped single tower cable-stayed bridge by adopting unstressed state method and reverse construction-forward installation iterative method, respectively. Both obtained reasonable cable forces during construction. To summarize, people's demand for bridge spans, economy, aesthetics and other needs and the booming development of modern construction technology have promoted the creation of asymmetrical irregular single tower cable-stayed bridges. Since it is a new type of bridge structure, the related research is very necessary and lacking, and the research on the optimization method of its construction ropes force is especially critical. Currently, scholars have studied cable-stayed bridges with different main tower morphologies and proposed applicable construction cable-stay optimization methods for specific engineering contexts. However, for the asymmetric fish-shuttle-shaped single tower cable-stayed bridges, its overall arc shape brings a lot of challenges in the analysis, and the related research on the optimization of the construction ropes force is relatively rare. The lack of relevant data and finite element modeling cannot provide an effective guide to the design, which has yet to be systematically investigated.

In view of this, based on a asymmetric fish-shuttle-shaped single tower cable-stayed bridge in China, finite element software Midas was adopted to build the model of it. Aiming at acquiring reasonable completed bridge cable forces, unstressed state method was put to use to optimize the cable force during construction and determined the reasonable construction state. The research results can provide reference for the design and optimization of similar projects.

2 Overview of Project

The bridge studied was a cable-stayed bridge in China with a single tower, double cable planes, and a tower-girder-pier consolidation system, which has a length of 386 m, and a four span continuous structure with a span arrangement of 256 m+50 m+40 m+40 m. The main tower was gate shaped horizontally, with a horizontal spacing of 36.5 m and a total tower height of 111 m. The numbering rule of the cables were as follows: the main-span cables numbered from right to left, with M1 on the far right and M19 on the far left; the side-span cables numbered from left to right, with S1 on the far left and S19 on the far right. The end support at the main span of the main girder was pm17, and the supports were numbered pm18, pm19, pm20, and pm21 from left to right. The layout of the bridge is shown in Fig. 1.

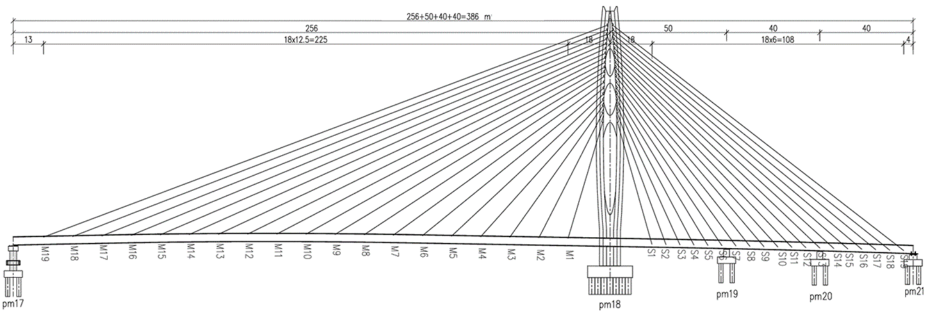

Fig. 1. Layout of the bridge

The main bridge was an asymmetrical single tower hybrid girder cable-stayed bridge, and the main girder adopted a hybrid girder structure with steel box girders on the main span and concrete box girders on the side span. The steel-cement bonding surface was set on the main-span side, 12 m from the centerline of the main tower. The fish-shuttle-shaped concrete tower was adopted in main tower, with hexagonal columns and an arch-shaped steel crossbeam at the top. The specific design parameters of materials are depicted in Table 1.

Table 1. Parameters of the main materials

Component	Material	Elastic modulus (GPa)	Unit weight ($kN \cdot m^{-3}$)
Steel box girder	Q345qc	206.0	78.5
Concrete box girder	C55	35.5	25.0
Main tower	C60	36.0	25.0
Arched steel cross-beam	Q345qc	206.0	78.5
Stay cable	1860 steel strand	195.0	78.5

The part of the main tower above the bridge deck was constructed by the bracket method and climbing mold method, in which the tower columns were constructed by climbing molds and the longitudinal tie girders between the tower columns, lower tower columns and girders were all constructed by brackets. Side-span concrete was constructed by bracket method, and the main-span steel girders were constructed by floating lift construction method. The main-span steel girders were divided into 19 construction sections from the main tower to the end support, corresponding to the cable numbers M1-M19. The cable were synchronized with the main-span steel box girder segments, and the side-span cables were installed accordingly. The cables were tensioned in the main tower and anchored in the main girders. The construction phases of the cable-stayed bridge were divided according to the actual construction sequence, and the construction phases are shown in Table 2.

Table 2. Division of construction phases

Construction phases	Contents of construction
CS1	Construction of main tower
CS2	Construction of side-span concrete box girder
CS3	Construction of Section 1 and tensioning of cables M1 and S1
CS4	Construction of Section 2 and tensioning of cables M2 and S2
CS5	Construction of Section 3 and tensioning of cables M3 and S3
CS6	Construction of Section 4 and tensioning of cables M4 and S4
CS7	Construction of Section 5 and tensioning of cables M5 and S5
CS8	Construction of Section 6 and tensioning of cables M6 and S6
CS9	Construction of Section 7 and tensioning of cables M7 and S7
CS10	Construction of Section 8 and tensioning of cables M8 and S8
CS11	Construction of Section 9 and tensioning of cables M9 and S9
CS12	Construction of Section 10 and tensioning of cables M10 and S10
CS13	Construction of Section 11 and tensioning of cables M11 and S11
CS14	Construction of Section 12 and tensioning of cables M12 and S12
CS15	Construction of Section 13 and tensioning of cables M13 and S13
CS16	Construction of Section 14 and tensioning of cables M14 and S14
CS17	Construction of Section 15 and tensioning of cables M15 and S15
CS18	Construction of Section 16 and tensioning of cables M16 and S16
CS19	Construction of Section 17 and tensioning of cables M17 and S17
CS20	Construction of Section 18 and tensioning of cables M18 and S18
CS21	Construction of Section 19 and tensioning of cables M19 and S19
CS22	Removal of brackets
CS23	Phase II paving of bridge deck
CS24	Simulation of 10-year shrinkage and creep of completed bridge

3 Finite Element Modeling

The finite element software Midas Civil was used to establish the spatial rod system model of the cable-stayed bridge, see Fig. 2. The whole bridge was divided into 509 nodes and 494 units, and the coordinate positions of the main girder and main tower units were established according to the actual design elevation. X-axis and Y-axis were parallel to the longitudinal section and cross-section of the main girder, respectively, and Z-axis was perpendicular to the plane of XY-axis. The main girder, the main tower and the bearing platform were simulated using girder units, where the main girders was simulated by the crane during the construction phase. For linear analysis, the cables was simulated by equivalent truss units, and for geometrically nonlinear analysis, the cables was simulated by elastic suspension units. The tower girder consolidation section of the main girders was rigidly connected to the main tower through multiple points to simulate tower-girder consolidation. The steel box girders and concrete box girders were simulated by sharing nodes between the steel and concrete box girders to simulate a steel-hybrid section. The nodes at the transition pier supports were constrained for translational displacements UY and UZ and corner displacements RX and RZ, and the nodes at the bottom of the main tower were constrained with solid ends. According to the coordinates of the anchorage points of the cable, rigid units were created to connect the diagonal cable to the main girder and the main tower.

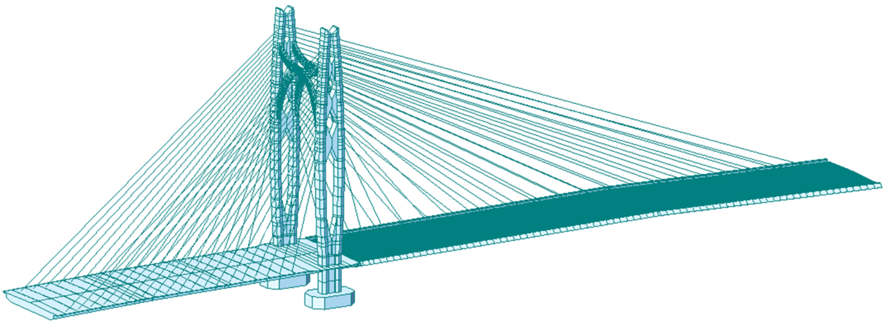

Fig. 2. Finite element model of the cable-stayed bridge

The minimum bending energy method was adopted to obtain the preliminary tension forces of the cable-stayed bridge. Aiming at minimizing the vertical displacement and bending moment of main girders, the influence matrix method was used to optimize the cable forces to obtain the initial tension cable force of the cable-stayed bridge. Finally, the cable forces were corrected by considering the sag effect, and its reasonable completed bridge tensioning force was determined. The optimization principle of the unstressed state method [18] is to disintegrate the structure in a linear state. As long as the length and unstressed curvature of each unit do not change, the restored structure will have the same internal force and line shape as the original structure regardless of the structural reorganization in any order, thus establishing a link between the construction phase of the cable-stayed bridge and the completed bridge phase. For the cable-stayed bridge system constructed in phases, unstressed state method is more applicable for optimization of construction cable force and has high computational efficiency. Therefore, the unstressed state method was adopted to optimize the construction cable force of the cable-stayed bridge in this paper. Firstly, the unstressed length under the reasonable completed bridge state was substituted into the Midas model, and the forward installation calculation was carried out in accordance with the construction steps. Then, the value of the completed bridge cable forces was replaced with the target cable forces after the construction stage of CS24 to correct the unstressed length, and the calculation was carried out in sequence for seven iterations. Eventually, the final construction tensioning forces were obtained, which were shown in Table 3.

Table 3. Final construction tensioning forces

Number of cables	Construction tensioning forces (kN)	Number of cables	Construction tensioning forces (kN)
S19	5758.9	M1	3750.4
S18	5541.5	M2	3469.6
S17	5183.7	M3	3060.5
S16	5136.5	M4	2696.7
S15	4908.9	M5	2474.7
S14	4851.0	M6	2121.1
S13	4722.3	M7	2466.1
S12	4515.8	M8	2220.9
S11	4376.4	M9	2502.1
S10	3987.5	M10	2625.1
S9	3728.6	M11	2694.6
S8	3525.6	M12	2865.5
S7	4353.6	M13	2853.2
S6	4547.3	M14	3792.8
S5	4529.3	M15	4420.9
S4	4601.6	M16	4167.1
S3	4805.0	M17	4097.6
S2	4904.3	M18	3937.8
S1	5036.9	M19	3712.4

4 Analysis of Optimization Result

4.1 Cable Force

The obtained reasonable bridge tension forces and construction tension forces are substituted into the model of Midas to obtain the corresponding cable forces under target completed bridge internal force state and construction calculated completed bridge internal force state, as shown in Fig. 3. It can be seen form the Fig. that the cable force under target completed bridge internal force state and construction calculated completed bridge state range from 2787.7 to 7026.0 kN and from 2620.5 to 6913.1 kN, respectively. Results indicate that the cable force under construction calculated internal force state is slightly lower than the target internal force state, which ensures the stability and safety of the cables during the construction process. The minimum and maximum cable force are M3 and S19 respectively, and there is no large sudden change in the adjacent cable force, and the overall cable force of the cable is uniformly distributed. The maximum difference between the cable force under target completed bridge internal force state and the construction calculated completed bridge internal force state is 6.00%. The average error of the cable force of entire bridge is 1.41%, and the average error of the cable force of main-span side and side span side are 0.99% and 1.83%, respectively. That is, through an effective tensioning can ensure that the error of completed bridge cable force under construction of the cable-stayed bridge with a span of nearly 400 m is small, and the use of unstressed state method to optimize the construction cable force of cable-stayed bridge can better meet the construction requirements.

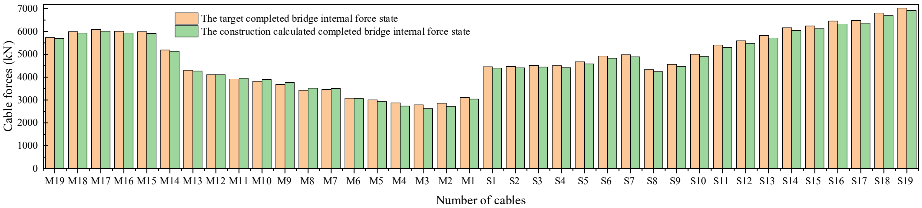

Fig. 3. Comparison of cable forces under the target completed bridge internal force state and the construction calculated completed bridge internal force state

4.2 Stress

The maximum stresses of the main tower at various construction phase can be seen in Fig. 4. As can be seen from the Fig., the maximum stress of the main tower increases as the construction process advances, while it decreases slightly during the construction phase of CS24, after taking into account the shrinkage and creep effects of concrete. Throughout the construction process, the maximum stress of the main tower ranges from 4.6 to 23.0 MPa, and peaks at 23.0 MPa during the construction phase of CS23, suggesting that it significantly lower than the design strength of concrete, and the stress state of main tower of cable-stayed bridge is safe enough.

The maximum stresses of side-span concrete girders at different construction phase are shown in Fig. 5. Overall, the maximum stress in the side-span concrete girders increases as the construction process progresses, whereas the maximum stress in the side-span concrete girders begins to decrease during the CS23 construction phase. In particular, the maximum stress in the side-span concrete girders is significantly reduced during the construction phase of CS24, taking into account the shrinkage and creep effects of the concrete. Throughout the construction process, the maximum stress of the side-span concrete girders ranges from 0 to 6.6 MPa, and peaks at 6.6 MPa during the construction phase of CS22. The peak stress is obviously lower than the design strength of concrete, showing the stress state of side-span concrete girders of cable-stayed bridge is safe.

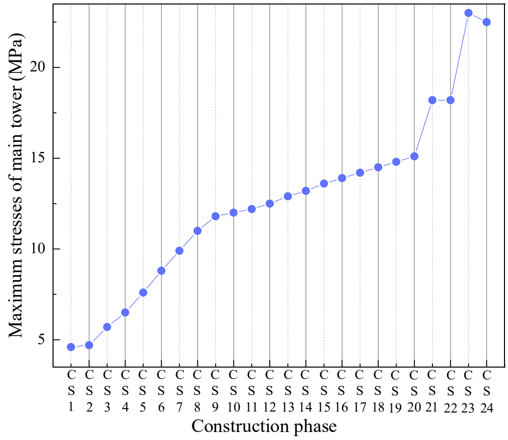

Fig. 4. Maximum stresses of main tower at various construction phase

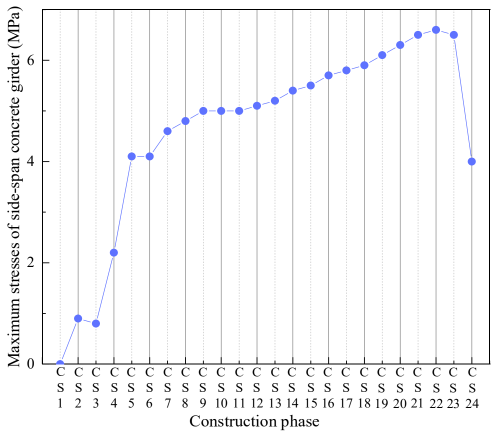

Fig. 5. Maximum stresses of side-span concrete girder at different construction phase

The maximum stresses of main-span steel box girders at each construction phase are depicted in Fig. 6. Results indicate that overall, with the advancement of construction process, the maximum stress of the main-span steel box girders increases, whereas it begins to decrease significantly during the CS23 construction phase. Throughout the construction process, the maximum stress of the main-span steel box girder ranges from 0 to 120.5 MPa, and peaks at 120.5 MPa during the construction phase of CS22, which is significantly lower than the design strength of steel, showing the safe stress state of main-span steel box girders of cable-stayed bridge.

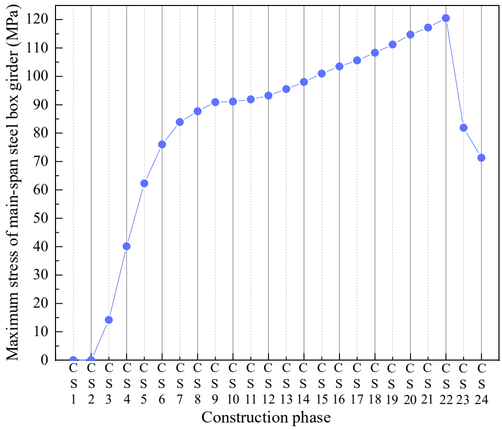

Fig. 6. Maximum stress of main-span steel box girder at each construction phase

4.3 Displacement

The maximum longitudinal displacements of the main tower at each construction phase are shown in Fig. 7. Overall, with the progressing of construction process, the maximum longitudinal displacement of the main tower increases. During the CS23 construction phase, namely after the Phase II paving of bridge deck, the maximum longitudinal displacement significantly reduces. Throughout the construction process, the maximum longitudinal displacement of the main tower ranges from 5.6 to 156.5 mm, and peaks during the construction phase of CS20, which can be ignored compared with the 111 m main tower, suggesting a reasonable deformation of main tower of cable-stayed bridge.

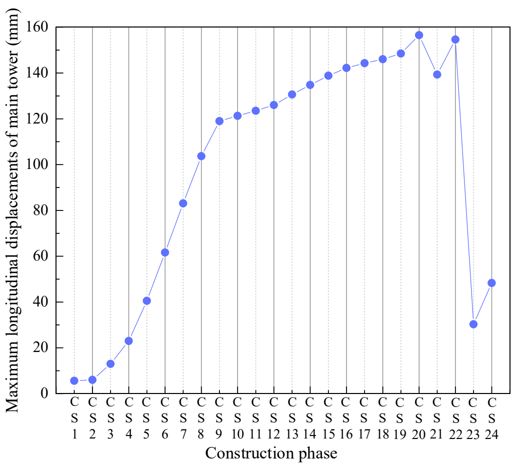

Fig. 7. Maximum longitudinal displacements of main tower at each construction phase

The maximum vertical displacements of the side-span concrete girders at different construction phase are depicted in Fig. 8. As can be seen from the Fig., the maximum vertical displacement of the side-span concrete girders remains relatively stable during the construction until the construction stage of CS22, i.e., after the removal of the bracing, the maximum vertical displacement is significantly reduced. Throughout the construction process, the maximum vertical displacement of the side-span concrete girders ranges from 0 to 20.8 mm, and peaks during the construction phase of CS22, which can be ignored compared with the 50 m span, indicating a reasonable deformation of side-span concrete girders of cable-stayed bridge.

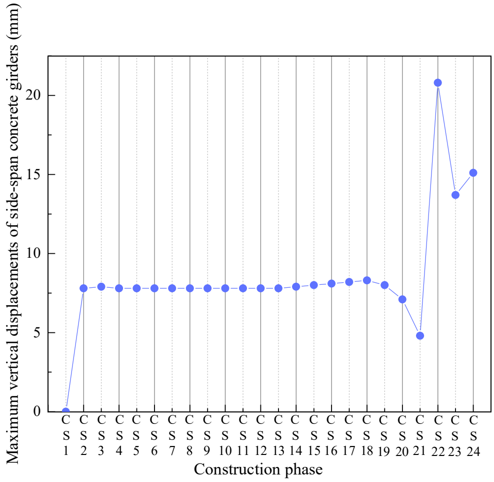

Fig. 8. Maximum vertical displacements of side-span concrete girders at different construction phase

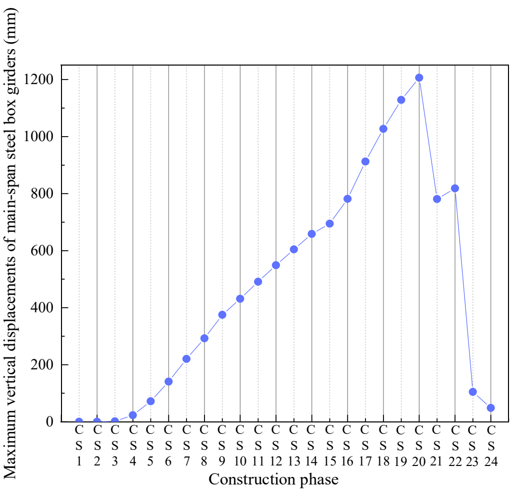

Fig. 9. Maximum vertical displacements of main-span steel box girders at various construction phase

The maximum vertical displacements of the main-span steel box girders at various construction phase are depicted in Fig. 9. Overall, as the construction process progresses, the maximum vertical displacement of the main-span steel box girders increases at first and then decreases. In construction phases CS21 and CS23, i.e., after the construction of the final section of steel box beam and Phase II paving of bridge deck, the maximum vertical displacement of main-span steel box girders decreases significantly. During the entire construction progress, the maximum vertical displacement of main-span steel box girders ranges from 0 to 1206.4 mm, and peaks at construction phase CS20. However, compared with 256 m span, the maximum displacement can be ignored, indicating a reasonable displacement of main-span steel box girders of cable-stayed bridge.

5 Conclusions

Based on an asymmetric cable-stayed bridge with fish-shuttle-shaped single tower in China, finite element software Midas Civil was adopted to build the model. The unstressed state method was used to optimize the construction cable forces of the cable-stayed bridge, and its reasonable construction state was determined. The main conclusions are as follows:

(1) The cable force under construction calculated completed bridge internal force state ranges from 2620.5 to 6913.1kN, which is slightly declined overall compared with that under target completed bridge internal force state, assuring the steady and safety of cables during construction. Maximum difference of 6.00% between the cable forces under target completed bridge internal force state and under construction calculated completed bridge internal force state. The average error of the cable forces of the whole bridge is 1.41%, including the average error of 0.99% of the main-span cable forces and 1.83% of the side-span cable forces. That is to say, through a single effective tensioning can ensure that the error of construction completed bridge cable force of cable stayed bridge with the span of nearly 400 m is relatively small, greatly improving its construction efficiency, so as to save time and labor costs. It is feasible and efficient to use the unstressed state method to optimize the construction cable force of asymmetric fish-shuttle-shaped single tower cable-stayed bridges, and future designers can give priority to this method when optimizing the construction cable-stay force of similar arc-shaped main tower cable-stayed bridges.

(2) The maximum stresses of main tower, side-span concrete girders and main-span steel box girders at each construction stage are 23.0, 6.6, and 120.5 MPa, respectively, which is significantly lower than the corresponding design strength of concrete and steel, showing a safe structural stress state of cable-stayed bridge. By comparing the maximum stresses in each structural part of a cable-stayed bridge at different construction phases, engineers can better predict and optimize the mechanical response of the structure at the design stage, ensure the safety of the construction process, and improve the economic efficiency.

(3) The maximum displacements of main tower, side-span concrete girders and main-span steel box girders at each construction stage are 156.5, 20.8, and 1206.4 mm,

respectively, which can be ignored compared with the structural dimension and layout, indicating a reasonable structural construction deformation of cable-stayed bridge. Comparing the maximum displacements of each structural part of a cable-stayed bridge at different construction phases can help engineers better predict and optimize the deformation response of the structure at the design stage, which can ensure the safety of the construction process, improving the economic efficiency. In addition, these data provide valuable lessons for optimizing the construction process of similar cable-stayed bridges in the future.

(4) The asymmetric fish-shuttle-shaped single tower cable-stayed bridge studied in this paper has a special overall curved shape which is not commonly seen, bring enormous difficulties worthwhile studying to the analysis of construction cable forces. The research results can provide relevant data and finite element model support for the optimization of the construction cable force of cable-stayed bridge with arc-shaped main tower. More researches on optimization of construction cable-stayed bridges with curved shapes (e.g., octopus-shaped and crab-shaped, etc.) can be carried out subsequently.

Acknowledgement

Funding: This research was funded by the project of cable force optimization method for asymmetric cable system of Chishi river cable-stayed bridge (No. HT-99982023-0558).
Conflicts of Interest: The authors declare that the research was conducted in the absence of any commercial or financial relationships that could be construed as a potential conflict of interest.

References

1. Atmaca, B. (2021) Size and post-tensioning cable force optimization of cable-stayed footbridge. Structures., 33: 2036–2049.
2. Ha, M.H., Vu, Q.A., Truong, V.H. (2018) Optimum design of stay cables of steel cable-stayed bridges using nonlinear inelastic analysis and genetic algorithm. Structures., 16: 288–302.
3. Editorial Department of China Journal of Highway and Transport. (2014) Review on China's Bridge Engineering Research: 2014. China Journal of Highway and Transport., 27(5): 1-96.
4. Lin, Y.P. (2004) Cable-stayed bridge. China Communications Press, Beijing, China.
5. Wang, X.M., Wang, H., Zhang, J., Sun, Y., Bai, Y.T., Zhang, Y.F., Wang, H.C. (2021) Form-finding method for the target configuration under dead load of a new type of spatial self-anchored hybrid cable-stayed suspension bridges. Eng. Struct., 227: 111407.
6. Shao, X.D. (2019) Bridge engineering. China Communications Press, Beijing, China.
7. Ye, H.Q. (2012) Cable force optimization of asymmetric cable-stayed bridge with single tower and single cable plane. Master's Thesis, Huazhong University of Science and Technology, Wuhan, China.
8. Shi, D.Z., Wang, J.F., Xiang, Y.Q., Xu, X. (2002) Optimum tensioning in construction state of cable-stayed bridge. China Journal of Highway and Transport, 2: 60-63.

9. Fu, Q., Li, Y.Q. (2012) Forward-back optimization method for determining construction cable force of cable-stayed bridge. Journal of Shijiazhuang Tiedao University(Natural Science), 25(3): 33-37.
10. Yan, D.H., Liu, G.D. (1999) Forward-iteration method for determining rational construction state of cable-stayed bridges. China Journal of Highway and Transport, 2: 61-66.
11. Tian, Y.W. (2021) Optimization of cable force of prestressed concrete cable-stayed bridge and stability analysis of the construction process. Master's Thesis, Kunming University of Science and Technology, Kunming, China.
12. Qin, S.Q. (2008) Application of unstressed state control method to calculation for erection of cable-stayed bridge. Bridge Construction, 38(2): 13-16+30.
13. Qin, S.Q. (2008) Unstressed state control method for bridges constructed in stages. Bridge Construction, 184(1): 8-14.
14. Shi, Y.J. (2024) Research on cable force optimization of unsymmetrical mixed beam single tower cable-stayed bridge. Master's Thesis, Anhui Jianzhu University, Hefei, China.
15. Liu, C.T. (2021) Practice of cable force optimization and construction monitoring for single-tower asymmetric cable-stayed bridge. Master's Thesis, Suzhou University of Science and Technology, Suzhou, China.
16. Wang, M., Yang, G.Z., Qin, Y.H., Wang, J.B., Cao, H. (2018) Study on installation calculation of cantilever assembly construction of single-pylon asymmetric cable-stayed bridge. Urban Roads Bridges&Flood Control, 12:127-130+134+17-18.
17. Xiao, Y.J. (2024) Research on cable force optimization and control of long-span asymmetric single-tower cable-stayed bridges. Master's Thesis, Yantai university, Yantai, China.
18. Li, B. (2022) Cable force optimization and construction simulation analysis of extradosed cable stayed bridge. Master's Thesis, Sichuan agricultural university, Chengdu, China.